Nanoscale

RSC Publishing

PAPER

View Article Online
View Journal | View Issue

Cite this: *Nanoscale*, 2013, **5**, 4816

Hierarchical ordering of amyloid fibrils on the mica surface†

Xingfei Zhou,[a] Yingying Zhang,[a] Feng Zhang,*[b] Saju Pillai,‡[c] Jianhua Liu,[a] Rong Li,[a] Bin Dai,[d] Bin Li[d] and Yi Zhang*[d]

Received 20th February 2013
Accepted 1st April 2013

DOI: 10.1039/c3nr00886j

www.rsc.org/nanoscale

The aggregation of amyloid peptides into ordered fibrils is closely associated with many neurodegenerative diseases. The surfaces of cell membranes and biomolecules are believed to play important roles in modulation of peptide aggregation under physiological conditions. Experimental studies of fibrillogenesis at the molecular level *in vivo*, however, are inherently challenging, and the molecular mechanisms of how surface affects the structure and ordering of amyloid fibrils still remain elusive. Herein we have investigated the aggregation behavior of insulin peptides within water films adsorbed on the mica surface. AFM measurements revealed that the structure and orientation of fibrils were significantly affected by the mica lattice and the peptide concentration. At low peptide concentration (~0.05 mg mL^{-1}), there appeared a single layer of short and well oriented fibrils with a mean height of 1.6 nm. With an increase of concentration to a range of 0.2–2.0 mg mL^{-1}, a different type of fibrils with a mean height of 3.8 nm was present. Interestingly, when the concentration was above 2.0 mg mL^{-1}, the thicker fibrils exhibited two-dimensional liquid-crystal-like ordering probably caused by the combination of entropic and electrostatic forces. These results could help us gain better insight into the effects of the substrate on amyloid fibrillation.

1 Introduction

The aggregation of soluble amyloid peptides into highly ordered fibrils has received considerable attention because of their relevance to many neurodegenerative diseases.[1–3] The well-known examples include amyloid-beta (Aβ) peptide and alpha-synuclein (α-Syn),[4–6] which are predominant in neuritic plaques of Alzheimer's and Parkinson's patients, respectively. These findings raise questions as to the factors driving and regulating related native functional proteins into insoluble fibrils. Numerous recent studies have made significant progress in understanding the peptide fibrillogenesis. It has been shown that amyloid fibril formation usually involves a nucleation-dependent polymerization mechanism consisting of an initial lag phase (nucleation) followed by a growth phase (elongation) and a steady state phase.[7,8] This progress has been suggested to be profoundly affected by the incubation temperature, interfaces, ionic strength and the addition of nanomaterials.[9–14]

One of the most puzzling phenomena in previous studies is that amyloid peptides could aggregate into fibrils *in vivo* at concentration 2–3 orders of magnitude lower than the critical value required for fibrillation in centrifuge tubes.[15–17] Several possible mechanisms have been proposed to interpret this discrepancy. The prevalent opinion is that surfaces from cell membranes and other macromolecules may play primary roles in modulating peptide aggregation under physiological conditions.[18,19] Indeed, within a living cell amyloid peptides are in very crowded environments owing to the existence of many volume-excluding macromolecules such as proteins, polysaccharides and lipids, which is often referred to as the molecular crowding effect.[20–22] Recently, the mutual interactions between membrane surfaces with Aβ and α-Syn have been revealed.[23,24] It has been observed in particular that the conformation shifted from a random coil free in solution to a membrane bound α-helix and then to β-sheet aggregation for Aβ and islet amyloid polypeptide (IAPP),[23,25,26] suggesting a membrane surface-mediated fibrillogenesis.

Due to the inherent challenges of experimental measurements in a crowded system *in vivo*, solid–liquid interfaces, therefore, have been frequently used to mimic the macromolecular crowding environments.[27–30] It has been generally recognized that substrates are capable of providing templates for the misfolding and ordering of amyloidogenic proteins into

[a]*Department of Physics, Ningbo University, Ningbo, 315211, China*

[b]*College of Life Sciences, Inner Mongolia Agricultural University, Hohhot, 010018, China. E-mail: Zhangfeng@imau.edu.cn*

[c]*Department of Mechanical and Manufacturing Engineering, Aalborg University, 9220, Aalborg, Denmark*

[d]*Shanghai Institute of Applied Physics, Chinese Academy of Sciences, Shanghai, 201800, China. E-mail: Zhangyi@sinap.ac.cn*

† Electronic supplementary information (ESI) available. See DOI: 10.1039/c3nr00886j

‡ Current address: Materials Science and Technology Division, National Institute for Interdisciplinary Science and Technology (NIIST), Kerala, 695019, India.

fibrils;[27,31–33] and the fibrillation progress remarkably depends on the compositions and physicochemical properties of substrates.[31,33–37] For example, the hydrophobic teflon surfaces could catalyze the insulin aggregation;[38] in contrast, the fibrillation process of IAPP was delayed by hydrophilic mica.[39] Despite the growing number of reports of peptide aggregation on solid–liquid interfaces, however, the molecular mechanisms of how substrates affect the structure and ordering of amyloid fibrils still remain elusive.

We have previously studied the diffusion and aggregation behavior of amyloid-like short peptides in two-dimensional water nanofilms condensed on mica under ambient conditions.[31,40–42] In this paper, we investigated the fibrillation of insulin at an interface of the mica substrate and thick water films achieved by incubating insulin peptides on the mica surface under high temperature and high humidity. We surprisingly found that the structure and orientation of insulin fibrils were profoundly influenced by the peptide concentration as well as the mica lattice underneath. Interestingly, the hierarchical ordering of insulin fibrils was observed, including threefold and two-dimensional liquid-crystal-like ordering of fibrils with a mean height of 1.6 and 3.8 nm, respectively.

2 Materials and methods

Chemicals and surface modification

Frozen insulin peptides were purchased from ProSpec with a purity of 98% and used without further purification. The insulin powder was dissolved in Milli-Q water (18.2 MΩ) to a concentration of 5.0 mg mL^{-1}. The pH of the solution was adjusted to 1.6 using 2 M HCl. The stock solution was stored at −20 °C and diluted to a designed concentration before use. In the control experiments, mica surfaces were modified with either NH_2- or CH_3-group by 3-aminopropyltriethoxysilane (APTES) (Sigma, Shanghai) and octadecyltrichlorosilane (OTS) (J&K Scientific Ltd) respectively before incubating insulin peptides on it. For NH_2-modification, a drop of freshly prepared aqueous solution of 0.5% APTES was placed on a mica surface. After 10 min incubation, the sample was extensively rinsed with Milli-Q water and dried with N_2 gas. Then the sample was heated at 100 °C for 1 hour. After cooling down it was stored in desiccators for use. Coating with the CH_3-group was achieved by immersing mica in an OTS–toluene solution (1 : 250 v/v) for 3 min, then the CH_3-modificed mica was rinsed with toluene before drying under a nitrogen stream. Contact angle measurement and XPS analysis confirmed the successful modification of the mica surface with CH_3- or NH_2-group (Fig. S1 and Table S1 in the ESI†).

Self-assembly of insulin fibrils

The preparation protocol for the fibrils formed on the mica surface within condensed water films was as follows: a drop of 10 μL peptide solution (pH: 1.6) with a designed concentration was deposited on mica (or CH_3-, NH_2-modified mica) with a surface area of ~0.8 × 0.8 cm^2, and spread uniformly on the whole mica surface. After dried in air, they were transferred into a sealed environment and incubated at 90 °C and ~100% relative humidity (RH) for a designed period of time.

To prepare aggregated insulin fibrils in solution, ~100 μL peptide solution (pH: 1.6) with a concentration of 0.5 mg mL^{-1} was incubated at 90 °C for 24 hours. Then, a drop of the solution was deposited on mica and dried with N_2 gas in air for AFM measurement.

Characterization of insulin fibrils

Tapping mode atomic force microscopy (AFM) images were collected using a NanoScope IIIa SPM (Veeco Instruments, Inc., Santa Barbara, CA) at room temperature and ~35% RH. Silicon cantilevers with a resonance frequency of ~260 kHz (RTESP, Veeco) were used for AFM imaging. The scanning rate was around 1–1.5 Hz. AFM data were analyzed with software NanoScope V5.31 and NanoScope Analysis V1.20.

The secondary structure of insulin fibrils formed in the bulk solution was probed at room temperature using a thermo nicolet infrared microscope (Nicolet 6700) equipped with a continuum infrared microscope accessory. A drop of the solution (2–3 μL) was deposited on a diamond sample holder and dried under infrared light at room temperature. The absorbance spectra of different samples were collected with a resolution of 8 cm^{-1}.

3 Results

Formation of two distinct types of insulin fibrils on mica

In our experiment, we used insulin as a model system. Initially, 10 μL of the peptide solution with a concentration of 0.2 mg mL^{-1} was deposited on a freshly cleaved mica surface. After dried in air, it was transferred into a sealed environment and incubated at 90 °C and ~100% RH for a designed period of time. During incubation the peptide molecules were able to diffuse and aggregate at the interface of the mica substrate and the condensed water films. The experimental procedures are schematically illustrated in Fig. 1. The subsequent *ex situ* AFM

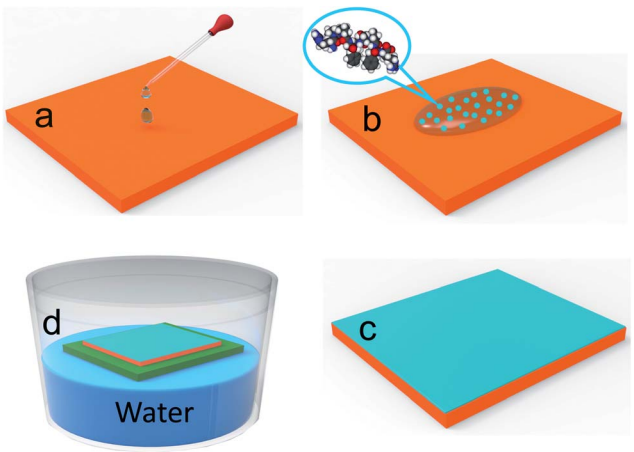

Fig. 1 Schematic description of the peptide sample preparation process including the preparation of freshly cleaved mica (a), deposition of a drop of peptide solution on mica (b), spreading and drying of the peptide solution on the mica surface (c) and incubation of the sample in a sealed environment at 90 °C and 100% RH (d).

imaging was operated under 35% RH to probe the morphology changes of the peptide assemblies. Interestingly, we observed a coexistence of two distinct types of insulin fibrils formed on the mica substrate after 25 hour incubation (Fig. 2). One type of insulin fibrils was short, straight, uniform and formed a very condensed network. The other type was curved and tangled with each other. They normally were "floating" on the top of the first type of insulin fibrils. For convenience, here we termed the fibrils at the bottom and on the top layers as Type I and Type II, respectively.

By zooming-in on a typical area more details of the fibril structure and orientation can be seen. At the bottom layer, insulin peptides grew as individual entities with inter-fibril angles of 60° or 120° (Fig. 2b and c) forming threefold symmetrical "epitaxial" patterns, which are very similar to the nanofilaments formed on mica as reported in our previous works and other research groups as well.[27,31,33,40–45] The oriented growth of insulin fibrils in this layer was most probably driven by the interaction between the peptides and the underlying mica lattice. To verify this speculation, insulin peptides were incubated on NH_2- and CH_3-modified mica surfaces respectively while keeping other experimental conditions constant. As expected, the correlation between the fibril orientation and the crystal lattice of mica was completely destroyed on two modified mica surfaces. We only observed non-uniform film-like structures formed by many irregular insulin fibrils on the NH_2-modified surface. While the CH_3-terminated surface showed disk-like aggregates of peptides with various sizes, no long separated fibrils were observed as shown in Fig. S2 (ESI),† which is comparable with the recent report by Moores *et al.*[46] Moreover, we also carried out another control experiment using the glass surface as a substrate. No ordered fibrils were observed (Fig. S3 in ESI†) after 25 hour incubation, further indicating that the oriented growth of insulin fibrils stems from the underlying mica lattice.

A statistical analysis was also conducted to obtain the height distribution of the two types of insulin fibrils. Fig. 3 shows that the rod-shaped Type I insulin fibrils were very uniform with a typical height of 1.6 ± 0.3 nm. In comparison, the height of the curly Type II fibrils reached 3.8 ± 1.1 nm. Although AFM images yield only topographic information, we

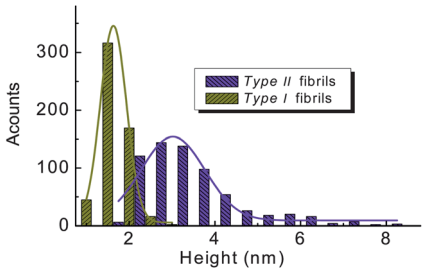

Fig. 3 Height distribution of the Type I and the Type II insulin fibrils. The mean height of these two type fibrils is 1.6 and 3.8 nm, respectively.

speculate that the difference in the apparent heights of the two types of insulin fibrils probably stemmed from the structural discrepancy. On further closer inspection of Type II fibrils, we found that some fibrils were formed *via* connection of small oligomeric units with varied sizes (Fig. 2c), differing from the straight or twisted morphology of fibrils formed in the bulk solution as illustrated in Fig. 4a,[47] where periodic height fluctuations along the contour of several fibrils can be clearly distinguished. Fig. 4b also shows the corresponding Micro-FTIR spectra of these fibrils, and the appearance of a peak at around 1631 cm^{-1} indicating the formation of the β-sheet structure.[47,48]

The *ex situ* time-lapse AFM images were further studied to reveal the evolution of peptide diffusion and self-assembly

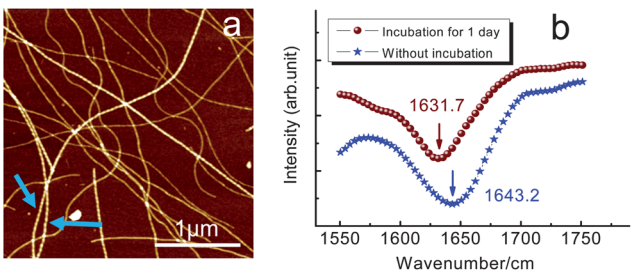

Fig. 4 AFM image of insulin fibrils formed in the bulk solution (a) and the corresponding Micro-FTIR spectra (b). Fibrils with periodically twisted morphologies are marked with colored arrows in (a). The appearance of the peak at about 1631 cm^{-1} in (b) indicated the formation of the β-sheet structure.

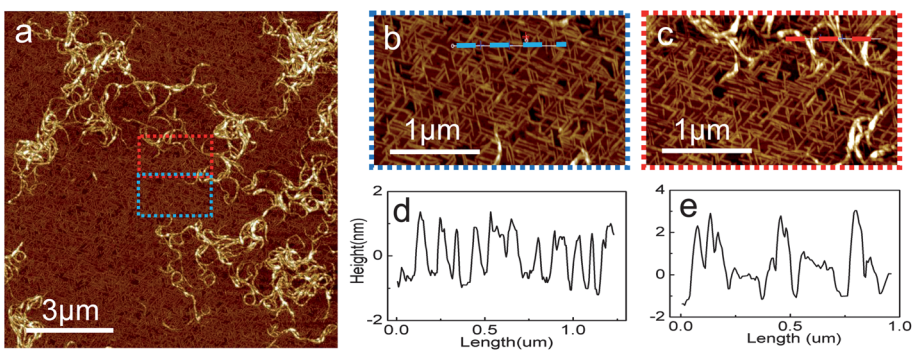

Fig. 2 AFM image of the insulin fibrils after incubation in a sealed environment at 90 °C and ~100% RH for 25 hours (a), (b) and (c) are magnified images of the areas as indicated by the colored rectangles in (a), (d) and (e) are the corresponding cross-section analysis of the fibrils marked with colored dotted lines in (b) and (c), respectively.

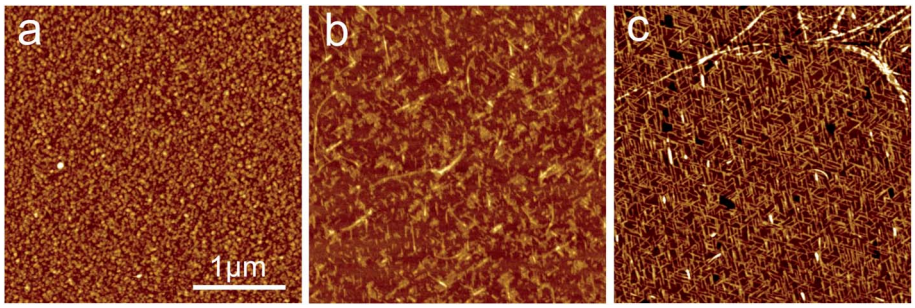

Fig. 5 A series of AFM images indicating the formation of insulin fibrils on a mica substrate at 90 °C and ~100% RH with the peptide concentration of 0.1 mg mL^{-1}. (a–c) Images obtained after 1, 10 and 20 hours, respectively. The scale bar in (a) applies to all images.

process. As illustrated in Fig. 5, at very beginning (~1 hour), the insulin peptides aggregated into oligomeric units, which may correspond to monomers, dimers, or small oligomers. With an increase of incubation time, more and more short and thin filaments appeared with certain orientation on the mica surface. After 20 hour incubation, a layer of very dense and orientationally ordered Type I insulin fibrils was observed, on top of which there appeared several longer and thicker Type II fibrils, indicating that the formation of Type I fibrils at the bottom was prior to Type II fibrils on its top. Although solid–liquid interfaces are often reported to catalyse the formation of amyloid fibrils due to an increase of the local peptide concentration, the growth rate of Type I fibrils is estimated to be only about 0.16 ± 0.07 nm min^{-1} from time-lapse AFM images, approximately 2–3 orders of magnitude slower than in the bulk solution.[49] It is likely because the peptide molecules bind to the mica surface in water films, resulting in a lower diffusion constant.

Two-dimensional liquid crystal-like ordering of Type II fibrils

Inspired by the concentration dependent liquid-crystalline behaviors of elongated biomolecular assemblies in solution,[50–53] we tried to realize a two-dimensional liquid crystal-like assembly of insulin fibrils on the mica surface, which has potential applications in functional nanomaterials. *Ex situ* AFM was used to monitor the buildup process of insulin peptides within water films with a series of different peptide concentrations. Fig. 6 illustrates the concentration dependence of the insulin fibrillation after 25 hour incubation at 90 °C and ~100% RH. Only a single layer of Type I fibrils was observed when the peptide concentration was 0.05 mg mL^{-1}. The insulin fibrils showed a high degree of homogeneity with a mean height of 1.6 nm. With an increase of the peptide concentration to a range of 0.2–2.0 mg mL^{-1}, an extra layer of longer and thicker Type II fibrils appeared. When the peptide concentration was further increased above 2.0 mg mL^{-1}, we remarkably observed a locally

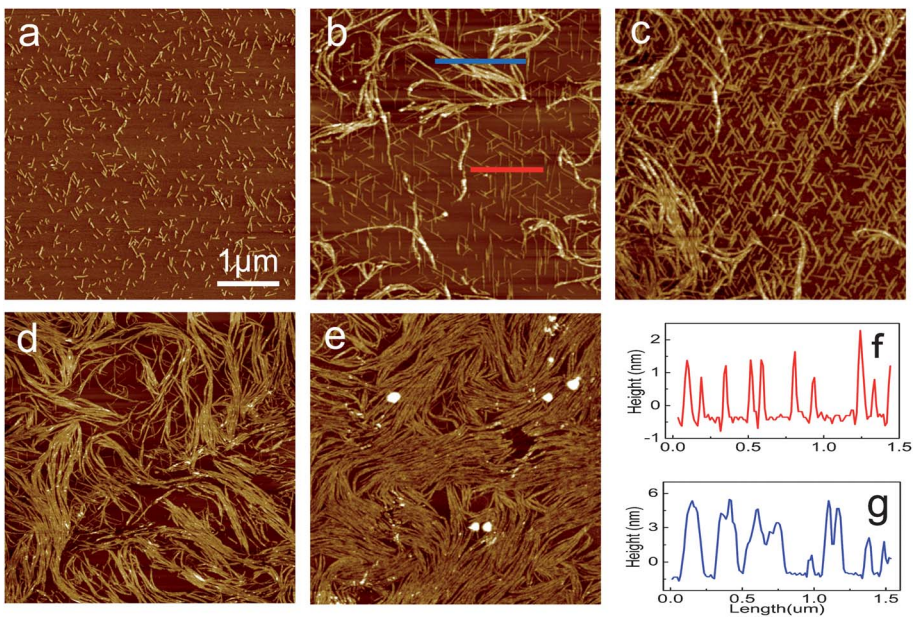

Fig. 6 Morphological and orientational differences between insulin fibrils formed on the mica surface at various concentrations as revealed by AFM. (a–e): 0.05, 0.2, 1.0, 2.0 and 3.0 mg mL^{-1}. (f) and (g) are cross-section analysis of the representative Type I and Type II fibrils marked with colored lines in (b). The scale bar in (a) applies to all images.

ordered Type II fibril "floating" on the top of the preformed Type I fibril layer as illustrated in Fig. 6e and f. Generally, the aspect ratio and the fibril concentration are the most important variables in solution for the presence of liquid-crystalline ordering such as smectic or nematic phases because of the entropic excluded-volume effects.[53–55] In our experiments, due to the highly effective concentration of insulin on mica and the charges on fibrils, the local ordering of Type II fibrils on the top layer was probably driven and regulated by the entropic force as well as electrostatic repulse interaction between fibrils.[56] In contrast, it is interesting to point out that the Type I insulin fibrils seem to be very similar in height, morphologies and orientation in a wide range of concentrations from 0.05 to more than 2 mg mL^{-1}, implying that the mica substrate might play a dominant role in the formation of Type I fibrils.

4 Discussion

Our results lead to a conclusion that the aggregation behavior of insulin peptides on the mica surface was critically dependent on the peptide concentration as schematically illustrated in Fig. 7. In our experiments, we should emphasize that the water films condensed on the mica surface provide an environment for insulin peptides to self-assemble. In general, a water film covers on the hydrophilic mica surface *via* keeping a dynamic balance between the evaporation and condensation of water molecules. The behavior of macromolecules in the water nanofilm on the mica surface in an ambient environment has been reported recently, for example, Emmanouil *et al.* observed the diffusion and aggregation of the poly(isoprene-*b*-ethylene oxide) block copolymer within interfacial water layers.[57] In our case the peptides on the mica substrate were kept in a sealed environment and incubated at 90 °C and ~100% RH, under which the water layers adsorbed on mica should be much thicker than those at room temperature due to the higher saturated vapor pressure. It is plausible to envisage that the Type I fibrils grew very close to the mica surface because the orientation of these fibrils was strongly modified by the mica lattice through electrostatic and van der Waals interactions.[58,59] From Fig. 5 and 6 it can be clearly seen that the Type II fibrils grew much faster than Type I. Hence, we infer that Type II fibrils were formed in less confined water layers with bulk-like features. A very interesting phenomenon is the concentration-dependent ordering of Type II fibrils floating on the underlayer of Type I fibrils. Generally, in solutions of highly concentrated fibrils, liquid-crystalline ordering is induced by the entropic excluded-volume (depletion) effect.[53,56] While in our case, electrostatic interactions between fibrils also contributed to the entropic ordering process. Similar ordering processes for charged species were also reported experimentally in the ordered complexation of DNA–liposome systems by X-ray scattering analysis.[60] To further explore the effect of concentration on Type II fibril ordering, the behavior of insulin peptides was also investigated within water films on mica with reduced thickness achieved by incubating the samples at lower temperature (70 °C) (Fig. S4 in ESI†). Although it is very tough to quantify the absolute thickness of the water film absorbed on mica under different temperatures, as expected, two hierarchically ordered layers of insulin fibrils were also present at a concentration of one order of magnitude lower than that for high temperature (90 °C), implying that the entropic force between fibrils at high concentration may play a critical role in orienting the fibrils.

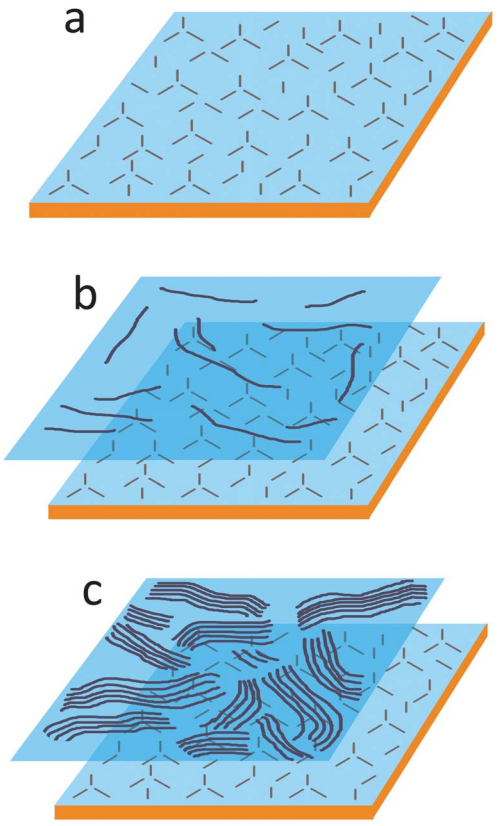

Fig. 7 Schematic illustration of fibril formation and ordering on the mica surface at different peptide concentrations. At low peptide concentration (~0.05 mg mL^{-1}), short and well oriented Type I fibrils were present on mica (a); at middle concentration, Type I and Type II fibrils co-existed (b); when the concentration was above 2.0 mg mL^{-1}, Type II fibrils exhibited two-dimensional liquid crystal-like ordering (c).

5 Conclusions

We found that the mica substrate has great influence on the insulin aggregation and fibrillation. The structure and orientation of fibrils were strongly dependent on the peptide concentration. At low peptide concentration (~0.05 mg mL^{-1}), short and threefold oriented Type I fibrils were present. With an increase of concentration, Type I and Type II fibrils co-existed on mica. Interestingly, when the peptide concentration was above 2.0 mg mL^{-1}, Type II fibrils formed a layer that exhibited two-dimensional liquid-crystal-like ordering. Our findings highlight the important roles that the mica substrate plays on the formation of amyloid fibrils, which could help us gain better insight into the effects of surfaces on the fundamental biochemical processes in a living cell. From a practical viewpoint, amyloid fibrils with the controlled orientational order

could potentially serve as scaffolds for biomineralization or as templates to direct the growth of another organic or inorganic structure.[45,61]

Acknowledgements

This work is funded by the National Natural Science Foundation of China (no. 11074137, 11274334, 21171086, 81160213), the Qianjiang Talent Project of Zhejiang Province (no. 2011R10084), the K. C. Wong Magna Fund in Ningbo University, and the National Basic Research Program of China (2013CB932800).

References

1 F. Chiti and C. M. Dobson, *Annu. Rev. Biochem.*, 2006, **75**, 333–366.
2 C. M. Dobson, *Nature*, 2003, **426**, 884–890.
3 C. X. Wang, A. H. Yang, X. Li, D. H. Li, M. Zhang, H. W. Du, C. Li, Y. Guo, X. B. Mao, M. Dong, F. Besenbacher, Y. Yang and C. Wang, *Nanoscale*, 2012, **4**, 1895–1909.
4 W. Hoyer, D. Cherny, V. Subramaniam and T. M. Jovin, *J. Mol. Biol.*, 2004, **340**, 127–139.
5 L. C. Serpell, *Biochim. Biophys. Acta*, 2000, **1502**, 16–30.
6 T. Kowalewski and D. M. Holtzman, *Proc. Natl. Acad. Sci. U. S. A.*, 1999, **96**, 3688–3693.
7 S. R. Collins, A. Douglass, R. D. Vale and J. S. Weissman, *PLoS Biol.*, 2004, **2**, 1582–1590.
8 M. Dong, M. B. Hovgaard, S. Xu, D. E. Otzen and F. Besenbacher, *Nanotechnology*, 2006, **17**, 4003–4009.
9 G. Yang, K. A. Woodhouse and C. M. Yip, *J. Am. Chem. Soc.*, 2002, **124**, 10648–10649.
10 H. Yang, S. Y. Fung, M. Pritzker and P. Chen, *Angew. Chem., Int. Ed.*, 2008, **47**, 4397–4400.
11 C. P. Shaw, D. Middleton, M. Volk and R. Lévy, *ACS Nano*, 2012, **6**, 1416–1426.
12 R. Paparcone, S. W. Cranford and M. J. Buehler, *Nanoscale*, 2011, **3**, 1748–1755.
13 J. Khandogin, J. Chen and C. L. Brooks III, *Proc. Natl. Acad. Sci. U. S. A.*, 2006, **103**, 18546–18550.
14 X. F. Zhou, J. H. Tan, L. F. Zheng, S. Pillai, B. Li, P. Xu, B. Zhang and Y. Zhang, *RSC Adv.*, 2012, **2**, 5418–5423.
15 P. Seubert, C. Vigo-Pelfrey, F. Esch, M. Lee, H. Dovey, D. Davis, S. Sinha, M. Schlossmacher, J. Whaley, C. Swindlehurst, R. McCormack, R. Wolfert, D. Selkoe, I. Lieberburg and D. Schenk, *Nature*, 1992, **359**, 325–327.
16 J. D. Harper and P. T. Lansbury Jr, *Annu. Rev. Biochem.*, 1997, **66**, 385–407.
17 A. Lomakin, D. S. Chung, G. B. Benedek, D. A. Kirschner and D. B. Teplow, *Proc. Natl. Acad. Sci. U. S. A.*, 1996, **93**, 1125–1129.
18 S. M. Butterfield and H. A. Lashuel, *Angew. Chem., Int. Ed.*, 2010, **49**, 5628–5654.
19 R. M. Murphy, *Biochim. Biophys. Acta*, 2007, **1768**, 1923–1934.
20 H. X. Zhou, G. Rivas and A. P. Minton, *Annu. Rev. Biophys.*, 2008, **37**, 375–397.
21 A. P. Minton, *J. Biol. Chem.*, 2001, **276**, 10577–10580.
22 D. A. White, A. K. Buell, T. P. Knowles, M. E. Welland and C. M. Dobson, *J. Am. Chem. Soc.*, 2010, **132**, 5170–5175.
23 J. A. Williamson, J. P. Loria and A. D. Miranker, *J. Mol. Biol.*, 2009, **393**, 383–396.
24 C. C. Jao, B. G. Hegde, J. Chen, I. S. Haworth and R. Langen, *Proc. Natl. Acad. Sci. U. S. A.*, 2008, **105**, 19666–19671.
25 C. Aisenbrey, T. Borowik, R. Byström, M. Bokvist, F. Lindström, H. Misiak, M. A. Sani and G. Gröbner, *Eur. Biophys. J.*, 2008, **37**, 247–255.
26 J. D. Knight, J. A. Hebda and A. D. Miranker, *Biochemistry*, 2006, **45**, 9496–9508.
27 C. Whitehouse, J. Y. Fang, A. Aggeli, M. Bell, R. Brydson, C. W. G. Fishwick, J. R. Henderson, C. M. Knobler, R. W. Owens, N. H. Thomson, D. A. Smith and N. Boden, *Angew. Chem., Int. Ed.*, 2005, **44**, 1965–1968.
28 F. Zaera, *Chem. Rev.*, 2012, **112**, 2920–2986.
29 M. Lepère, C. Chevallard, J. F. Hernandez, A. Mitraki and P. Guenoun, *Langmuir*, 2007, **23**, 8150–8155.
30 S. Zhang, S.-J. Cho, K. Busuttil, C. Wang, F. Besenbacher and M. Dong, *Nanoscale*, 2012, **4**, 3105–3110.
31 S. G. Kang, H. Li, T. Huynh, F. Zhang, Z. Xia, Y. Zhang and R. Zhou, *ACS Nano*, 2012, **6**, 9276–9282.
32 H. Yang, S. Y. Fung, M. Pritzker and P. Chen, *J. Am. Chem. Soc.*, 2007, **129**, 12200–12210.
33 C. R. So, Y. Hayamizu, H. Yazici, C. Gresswell, D. Khatayevich, C. Tamerler and M. Sarikaya, *ACS Nano*, 2012, **6**, 1648–1656.
34 F. Zhang, H. N. Du, Z. X. Zhang, L. N. Ji, H. T. Li, L. Tang, H. B. Wang, C. H. Fan, H. J. Xu, Y. Zhang, J. Hu, H. Y. Hu and J. H. He, *Angew. Chem., Int. Ed.*, 2006, **45**, 3611–3613.
35 M. I. Smith, J. S. Sharp and C. J. Roberts, *Biophys. J.*, 2007, **93**, 2143–2151.
36 L. Shen, T. Adachi, B. D. Vanden and X. Y. Zhu, *J. Am. Chem. Soc.*, 2012, **134**, 14172–14178.
37 A. Keller, M. Fritzsche, Y. P. Yu, Q. Liu, Y. M. Li, M. Dong and F. Besenbacher, *ACS Nano*, 2011, **5**, 2770–2778.
38 V. Sluzky, J. A. Tamada, A. M. Klibanov and R. Langer, *Proc. Natl. Acad. Sci. U. S. A.*, 1991, **88**, 9377–9381.
39 C. Goldsbury, J. Kistler, U. Aebi, T. Arvinte and G. J. S. Cooper, *J. Mol. Biol.*, 1999, **285**, 33–39.
40 H. Li, F. Zhang, Y. Zhang, M. Ye, B. Zhou, Y. Z. Tang, H. J. Yang, M. Y. Xie, S. F. Chen, J. H. He, H. P. Fang and J. Hu, *J. Phys. Chem. B*, 2009, **113**, 8795–8799.
41 M. Xie, H. Li, M. Ye, Y. Zhang and J. Hu, *J. Phys. Chem. B*, 2012, **116**, 2927–2933.
42 M. Ye, Y. Zhang, H. Li, M. Xie and J. Hu, *J. Phys. Chem. B*, 2010, **114**, 15759–15765.
43 X. Yu, Q. Wang, Y. Lin, J. Zhao, C. Zhao and J. Zheng, *Langmuir*, 2012, **28**, 6595–6605.
44 A. Karsai, L. Grama, U. Murvai, K. Soos, B. Penke and M. S. Z. Kellermayer, *Nanotechnology*, 2007, **18**, 345102.
45 T. Akutagawa, T. Ohta, T. Hasegawa, T. Nakamura, C. A. Christensen and J. Becher, *Proc. Natl. Acad. Sci. U. S. A.*, 2002, **99**, 5028–5033.

46 B. Moores, E. Drolle, S. J. Attwood, J. Simons and Z. Leonenko, *PLoS One*, 2011, **6**, e25954.
47 R. Jansen, W. Dzwolak and R. Winter, *Biophys. J.*, 2005, **88**, 1344–1353.
48 J. Brange, L. Andersen, E. D. Laursen, G. Meyn and E. Rasmussen, *J. Pharm. Sci.*, 1997, **86**, 517–525.
49 T. Ban, D. Hamada, K. Hasegawa, H. Naiki and Y. Goto, *J. Biol. Chem.*, 2003, **278**, 16462–16465.
50 W. C. Pomerantz, V. M. Yuwono, C. L. Pizzey, J. D. Hartgerink, N. L. Abbott and S. H. Gellman, *Angew. Chem., Int. Ed.*, 2008, **47**, 1241–1244.
51 A. M. Corrigan, C. Müller and M. R. Krebs, *J. Am. Chem. Soc.*, 2006, **128**, 14740–14741.
52 T. P. Knowles, T. W. Oppenheim, A. K. Buell, D. Y. Chirgadze and M. E. Welland, *Nat. Nanotechnol.*, 2010, **5**, 204–207.
53 J. Herzfeld, *Acc. Chem. Res.*, 1996, **29**, 31–37.
54 M. Adams, Z. Dogic, S. L. Keller and S. Fraden, *Nature*, 1998, **393**, 349–352.
55 M. Lepère, C. Chevallard, J. F. Hernandez, A. Mitraki and P. Guenoun, *Langmuir*, 2007, **23**, 8150–8155.
56 P. J. Yoo, K. T. Nam, J. Qi, S. K. Lee, J. Park, A. M. Belcher and P. T. Hammond, *Nat. Mater.*, 2006, **5**, 234–240.
57 G. Emmanouil, P. Stergios and K. Vasileios, *Macromolecules*, 2008, **41**, 4313–4320.
58 C. M. Roth and A. M. Lenhoff, *Langmuir*, 1995, **11**, 3500–3509.
59 J. Chun, J. L. Li, R. Car, I. A. Aksay and D. A. Saville, *J. Phys. Chem. B*, 2006, **110**, 16624–16632.
60 J. O. Radler, I. Koltover, T. Salditt and C. R. Safinya, *Science*, 1997, **275**, 810–814.
61 E. Thormann, H. Mizuno, K. Jansson, N. Hedin, M. S. Fernández, J. L. Arias, M. W. Rutland, R. K. Pai and L. Bergström, *Nanoscale*, 2012, **4**, 3910–3916.

